BIFURCATION MECHANISMS AND ATMOSPHERIC BLOCKING

Erland Källén

ECMWF

Abstract

The bifurcation properties of low order, barotropic models with orographic and a Newtonian type of vorticity forcing are reviewed. The low order model results that multiple equilibria develop as a result of a sufficiently strong wave, orographic forcing and that a suitably positioned wave vorticity forcing can enhance this bifurcation mechanism are verified with a high resolution, spectral model. The high resolution model is integrated in time to find stable steady-states. Bifurcations into multiple equilibria appear as sudden jumps in the amplitudes of the model components, when the forcing is slowly changing in time.

Diagnostic studies of the mountain torque and the eddy activity in the Northern Hemisphere during winter are compared with the occurrence of blocked flows to support the blocking mechanism originally proposed by Charney and DeVore (1979).

1. INTRODUCTION

In recent years there has been a renewed interest in the study of low-order systems to gain some insight into nonlinear mechanisms present in the atmosphere. The basic procedure used when studying a low-order system is to expand the space dependent quantities into a series of orthogonal functions and to truncate this expansion by just retaining a few components. Each component is thought of as representing a certain scale of motion and, by inserting the truncated expansion into an equation of motion, one can study the nonlinear interactions between the scales considered. One thus neglects

all interactions with spectral components not taken into account. This is of course a serious limitation of low-order systems, but it is nevertheless believed that a study of such systems is one way of getting an insight into the nonlinear mechanisms present in the atmosphere. To verify results found with a low-order model one should also perform experiments with a high-resolution, fully nonlinear model. These experiments must, however, be guided by the qualitative properties of the low-order systems.

To study the effect of orographic forcing on the nonlinear energy transfer between the larger scales of motion, Charney and DeVore (1979) (hereafter called CdV) extended Lorenz's (1960) barotropic β-plane model to include orographic forcing. With a low-order system they showed that for a given forcing it was possible for the flow to arrange itself in several equilibrium states, some stable and some unstable. The multiplicity of equilibrium states is associated with the resonance occurring when the Rossby wave, generated by the zonal flow over the orography, becomes stationary. Through the nonlinear interaction between the zonal flow and the wave components of the flow and due to the orography, the components can arrange themselves in two stable equilibria, one close to resonance with a large amplitude wave and a weak zonal flow, the other with a strong zonal flow and a weaker wave component. The large amplitude wave flow may be associated with a blocked flow in the atmosphere.

This result was first derived for a β-plane, channel model with reflecting side walls, but later studies by Davey (1980,1981) and Källén (1981) have shown that the same type of mechanism can be found with an annular or a spherical geometry. Trevisan and Buzzi (1980) also showed the same phenomenon using a different expansion method on a β-plane geometry.

The basic equation used for the models of all these studies is the quasi-geostrophic, barotropic vorticity equation with linear dissipation, a Newtonian type of vorticity forcing and orographic forcing. In a non-dimensional form this equation is

$$\frac{\partial \zeta}{\partial t} = J(\zeta + f + h, \psi) + \varepsilon(\zeta_E - \zeta) \qquad (1)$$

where ζ is the non-dimensional vorticity, f is the planetary vorticity, ζ_E the vorticity forcing, ψ the stream function and h is a parameter related to the orographic effects. The non-dimensional time is given by t and ε is the dissipation rate. The orographic forcing may be introduced as a forced vertical velocity of the lower boundary in an equivalent barotropic model, in which case h is related to a dimensional mountain height m via

$$h = C \cdot \frac{m}{H} \qquad (2)$$

where H is the scale height of the equivalent barotropic atmosphere and C is a constant which depends on the equivalent barotropic assumption. For normal atmospheric conditions the constant C is approximately equal to one. For details of the derivation of Eq.(1) see Källén (1981).

The nonlinearity of the model is contained in the term involving the Jacobian ($J(\zeta + f+h, \psi)$), and one way of investigating the nonlinear properties of this model is to expand the space dependent variables in a series of orthogonal functions, $F_\gamma(\underline{x})$, where $\underline{x}$ is the space vector. It is convenient to choose the F_γ's to be eigenfunctions of the Laplacian operator, because $\zeta = \nabla^2\psi$. The exact functional form of the F_γ's of course depends on the geometry of the model and the boundary conditions.

The variables to be expanded are the vorticity (also gives the streamfunction), vorticity forcing and the orography. The expansion may be

written

$$\begin{pmatrix} \zeta \\ \zeta_E \\ h \end{pmatrix} = \sum_\gamma \begin{pmatrix} \zeta_\gamma(t) \\ \zeta_{E,\gamma} \\ h_\gamma \end{pmatrix} F_\gamma(\underline{x}) \tag{3}$$

For a β-plane, channel model trigonometric functions can be used and $F_{m,n}(x,y) = e^{i(mx+ny)}$, x and y being the Cartesian coordinates (CdV). In an annular geometry, Bessel functions are involved (see Davey, 1981) and on the sphere the F_γ's may be written

$$F_{m,n}(\mu,\lambda) = P_n^m(\mu)\, e^{im\lambda} \tag{4}$$

where μ is the sine of latitude (ϕ), λ is the longitude and $P_n^m(\mu)$ are associated Legendre functions. Most of the results discussed in this paper will refer to a spherical geometry as in Källén (1981) and thus the expansion functions given by Eq.(4) are the appropriate ones.

A low-order model may be formulated by inserting the expansion Eq.(3) in the model Eq.(1) and truncating the expansion at a very low order just leaving a few components to describe the fluid motion. Each component may be thought of as describing a certain scale of motion and only the nonlinear interactions between the scales involved in the low order system are taken into account.

To study the effects of the orography on the interaction between the waves and the mean zonal flow, at least one purely zonal component and two wave components have to be included. The mathematical structure of such a minimal system is independent of the geometry and multiple equilibrium states may be found even in such a simple model, as first pointed out by CdV. When

additional components are included the geometry will affect the structure of the equations, but the basic mechanism for the formation of multiple equilibrium states still remains. In the following section a minimal system will be analyzed, following the basic idea of CdV. Section 3 will deal with a combination of orographic and direct wave vorticity forcing as discussed by Källén (1981). The direct wave vorticity forcing is thought to represent the time mean effect of the small scale baroclinic eddies on the long waves in the atmosphere. In Section 4 a verification of some of the drastic assumptions made when dealing with low-order models will be made and in Section 5 we will try to relate the bifurcation properties of the simplified models to diagnostic studies of the atmosphere in connection with blocking events.

2. WAVE-MEAN FLOW INTERACTIONS VIA THE OROGRAPHY

The simplest possible low-order model in which one may investigate the nonlinear coupling between the zonal mean flow and the eddies through the effect of the orography, is a model which involves one component describing a purely zonal flow and two components describing the phase and amplitude of a wave. On the sphere the streamfunction may thus be written

$$\psi = -u_o(t)\ P_1(\mu) + (x_1(t)\ \cos\ell\lambda + y_1(t)\ \sin\ell\lambda) P_n^{\ell}(\mu)$$

where u_o, x_1 and y_1 are the time dependent amplitudes of each flow component. To drive the zonal flow, a vorticity forcing is introduced in the $P_1(\mu)$ component with an amplitude, u_{oE}. The orography is assumed to be present with an amplitude, h_1, in the $\cos\ell\lambda P_n^{\ell}(\mu)$ component. Inserting these expansions of the stream function, vorticity forcing and the orography into the barotropic vorticity equation (1), a set of three ordinary differential equations governing the time evolution of the model is obtained,

$$\begin{aligned}
\dot{u}_o &= h_1\ \delta_1\ y_1 && + \varepsilon(u_{oE} - u_o) \\
\dot{x}_1 &= && (\beta - \alpha\ u_o) y_1 \quad - \varepsilon x_1 \qquad (5) \\
\dot{y}_1 &= -h_1\ \delta_2\ u_o - (\beta - \alpha\ u_o) x_1 && - \varepsilon y_1
\end{aligned}$$

The coefficients appearing in (5) are defined

$$\alpha = \sqrt{3}\ell\ [1-2/n(n+1)]\ ,\ \beta = \frac{2\ell}{n(n+1)}\ ,\ \delta_1 = \frac{\sqrt{3}}{4}\ell,\ \delta_2 = \frac{\sqrt{3}\ell}{n(n+1)}\ .$$

These expressions for the coefficients have been derived for a spherical geometry, but in fact the structure of the equations is exactly the same for

a β-plane or an annular geometry, the only difference between the different geometries lie in the expressions for and values of the coefficients. The results shown in this section, may thus equally well be applied to the other types of geometry.

To investigate the mathematical properties of the nonlinear system of equations (5), we first determine the steady-state values of u_o, x_1 and y_1. Setting the time derivatives equal to zero and solving the resulting system of equations for one of the steady-state amplitudes (u_o), we arrive at the following equation in $\bar{u}_o$ (hereafter an overbar will denote a steady-state amplitude)

$$\bar{u}_o^3 - \bar{u}_o^2 \left(u_{oE} + \frac{2\beta}{\alpha}\right) + \frac{\bar{u}_o}{\alpha^2}\left[\delta_1\delta_2 h_1^2 + \varepsilon^2 + \beta^2 + 2\beta\, u_{oE}\right] = u_{oE}\,\frac{(\varepsilon^2 + \beta^2)}{\alpha^2} \tag{6}$$

which also may be written

$$u_{oE} = \frac{\delta_1\delta_2\, h_1^2\, \bar{u}_o}{\varepsilon^2 + (\beta - \alpha\bar{u}_o)^2} + \bar{u}_o \tag{7}$$

The polynomial form (6) of the steady-state equation shows that we can at the most have three steady-states for certain values of the forcing parameters. The other form of the steady-state equation, (7), allows us to investigate by graphical methods how the number of steady-states varies with the forcing parameters. Note that on the left hand side of (7), u_{oE} is a velocity. This velocity is the purely linear response of the u_o-component when there is no orography.

The example chosen to illustrate Eq. (7) is one in which ℓ=3 and n=4. This implies an orography with a zonal wavenumber three and a maximum in

mid-latitudes. Fig. 1 is a plot of the curves given by Eq.(7) for some values of h_1. Both axes are given in non-dimensional and dimensional units. The dimensional units are m/s and correspond to the windspeed of the u_o component at 45° latitude.

The curve in Fig. 1 for $h_1 = 0$ is a straight line and for increasing values of h_1 we obtain a family of curves, some having a section with a negative slope. As each point on the curves represents a steady-state of the system given by Eqs. (5), a negatively sloping section of a curve implies that within a certain forcing parameter (u_{oE}) interval it is possible to have three steady-states. Taking as an example the curve for $h_1 = 0.20$ it can be seen from Fig. 1 that in the interval $0.135 < u_{oE} < 0.158$ three steady-states exist. The stability properties of each steady-state are found by linearising Eq. (5) around each steady-state, and finding the eigenvalues of the linearized equations. An investigation of this kind gives stability properties as indicated by full (stable) and dashed (unstable) lines in Fig. 1. In Fig. 2 it may also be seen that the bifurcation from one to three steady-states occurs for a value of h_1 somewhere between 0.10 and 0.15.

The possibility of having two stable equilibrium states for constant values of the forcing parameters is due to the nonlinear coupling between the zonal flow and the waves. The coupling by itself, however, without the effect of the orography, does not give rise to multiple steady-states in Eq.(5). It is the influence of the orography which is crucial in creating an instability which gives the possibility of having multiple steady-states. CdV called this a form drag instability, where the form drag refers to the effect of the orography in this simple model.

One of the stable steady-states is close to a resonant flow configuration, and in this steady-state the wave component has a high amplitude. The phase of the wave is such that there is a high drag across the orographic ridges

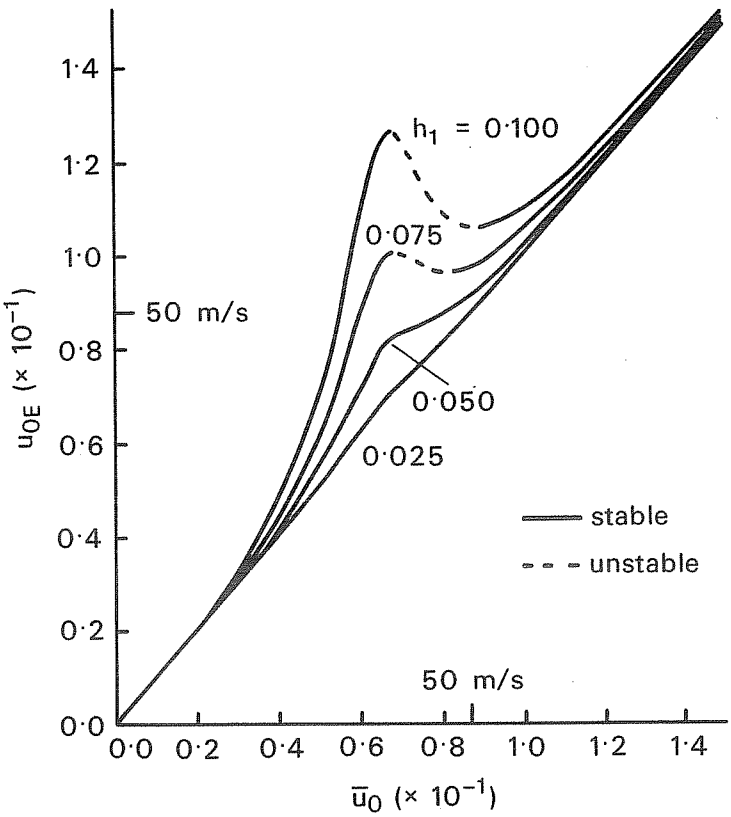

Fig. 1 Steady-state curves for the low order model of section 2 with different values of the orographic parameter. The horizontal axis gives the amplitude of the $\bar{u}_o$-component, both in non-dimensional and dimensional units. On the vertical axis the forcing is also given in both units. The dimensional units are the flow velocity at 45° latitude. Each curve corresponds to a certain value of the orographic parameter, h_1, and a numerical evaluation of the eigenvalues shows stability properties as indicated by full (stable) and dashed (unstable) lines. For further explanations, see text.
Parameter values: $\varepsilon = 0.06$, $\ell = 3$, $n_1 = 4$.

and thus energy is transferred from the zonal forcing, via the effect of the orography, to the wave components of the flow. In Fig. 1 this type of a steady-state falls on the left hand part of the diagram where the response in the zonal component (u_o) is much less than the forcing.

The steady-states on the right hand side of the unstable region have a more intense zonal flow and a less marked wave component. In these steady-states the orographic drag is much lower, both due to the lower amplitude of the wave component and a different phase of the wave.

The steady-state with a high wave amplitude may be associated with a blocked flow in the atmosphere. The wave ridge occurs downstream of the orographic ridge, and the persistence of blocking ridges in the atmosphere may be due to the stable wave-mean flow interaction described by this simple model. The model also predicts that there may be another stable flow configuration without a high amplitude wave, but a much more pronounced zonal flow. Which one of these steady-states the flow settles into is crucially dependent on the initial state of the flow. CdV offered this feature as a possible explanation for the observed variability in the frequency of the occurrence of blocked flows.

3. A COMBINATION OF WAVE VORTICITY AND OROGRAPHIC FORCING

In the model described in the previous section, the waves of the flow are only due to the interaction between the zonal flow and the orography. In the atmosphere there are numerous other processes which generate waves and in midlatitudes the most important one is the baroclinic instability process. Baroclinic waves have a characteristic wavelength which is shorter than the scales involved in the low order models of this study, but seen as an effect on the time mean flow the energy generated by baroclinically unstable waves on the shorter scales is transported in the spectrum through nonlinear processes and thus also exports energy to the longer waves (Saltzmann, 1970 and Steinberg et al, 1971). In a barotropic model it is impossible to describe these baroclinic effects explicitly, but one may be able to take the long wave effect into account by introducing a wave vorticity forcing in the same components as the orography. The wave vorticity forcing should thus be seen as the time mean effect of cyclone waves rather than a direct diabatic heating.

A wave vorticity forcing can easily be introduced into the low order model of the previous section by adding εx_{1E} and εy_{1E} to the right hand sides of the equations for $\dot{x}_1$ and $\dot{y}_1$ of Eq.(5). The steady-states may be analyzed in the same way by writing the steady-state equation in terms of the zonal forcing (u_{oE}) as a function of the zonal response (u_o) with the orography (h_1), the amplitude ($\sqrt{x_{1E}^2 + y_{1E}^2}$) and the phase ($\tan^{-1}\frac{y_{1E}}{x_{1E}}$) of the wave vorticity forcing as parameters. In Källén (1981) this was done, but with a sightly more complicated model. Two extra wavecomponents and one extra zonal component was included to take into account some of the interactions with unforced parts of the spectrum. It is still possible to solve for the steady-states analytically in such a model according to the procedure given in Källén (1981). We will not go into any detail here regarding the solution method, but only display some of the results.

The streamfunction expression used in the examples is

$$\psi(\mu, \lambda, t) = - u_o(t)\ P_1(\mu) + z(t)\ P_3(\mu)$$

$$+ \ (x_1(t) \cos 3\lambda + y_1(t) \sin 3\lambda)\ P_4^3(\mu) +$$

$$+ \ (x_2(t) \cos 3\lambda + y_2(t) \sin 3\lambda)\ P_6^3(\mu)$$

and the vorticity forcing is given by

$$\psi_E(\mu,\lambda) = - u_{oE}\ P_1(\mu) +$$

$$+ \quad (x_{1E} \cos 3\lambda + y_{1E} \sin 3\lambda)\ P_4^3(\mu) \ .$$

The orography is the same as in the previous section,

$$h = h_1 \cos 3\lambda\ P_4^3(\mu)$$

The low order system is thus made up of six ordinary differential equations, which govern the time evolution of the model. Because of the choice of components, no direct wave-wave to wave interactions are allowed but energy transfer from one wave-component to the other may take place via the zonal flow. The zonal component with the amplitude z describes a sheared zonal flow and it is via this zonal component that energy may be transferred through flow-flow interactions from the forced to the unforced wave components.

A plot of the steady-states of the system is given in Fig. 2. On the horizontal axis the steady-state response is given in terms of the amplitude of the sheared zonal component, z. The vertical axis gives the zonal momentum forcing, u_{oE}.

The orographic forcing is fixed at a value of 0.05 while the wave vorticity forcing has a varying amplitude, but the phase in relation to the orography is fixed. Multiple steady-states of the system are identified in the figure by the condition that a horizontal line should have multiple intersections with one of the steady-state curves. The forcing parameters are in a range where multiple steady states are just possible, i.e. close to the first bifurcation point. For smaller values of the forcing parameters the nonlinear system behaves quasi-linearly, with just one steady state for a certain value of the forcing parameters. By linearizing the system around a steady-state and computing the eigenvalues of the matrix governing the linearized motion around each of the steady-states, stability properties are found as indicated in Fig. 2. It may be noted that no Hopf-bifurcations (see Marsden and McCracken, 1979) indicating the existence of limit-cycles around the steady-states have been found in this low order model for reasonable values of the forcing parameters.

For the curve marked I in Fig. 2 the wave vorticity forcing is set to zero and the only forcing of the model is in the orography and the zonal momentum. For the orography height chosen in Fig. 2 there is only one, stable steady-state for all values of the zonal momentum forcing. For higher values of the orographic parameter multiple steady-states are possible within certain ranges of values of the zonal momentum forcing. For further details of this, see Källén (1981). Another way of obtaining a region of multiple equilibria is to include vorticity forcing in one of the wave components and this is shown with steady state curve II in Fig.2. The phase of the wave vorticity forcing is -90°, i.e. positive (cyclonic) vorticity forcing on the

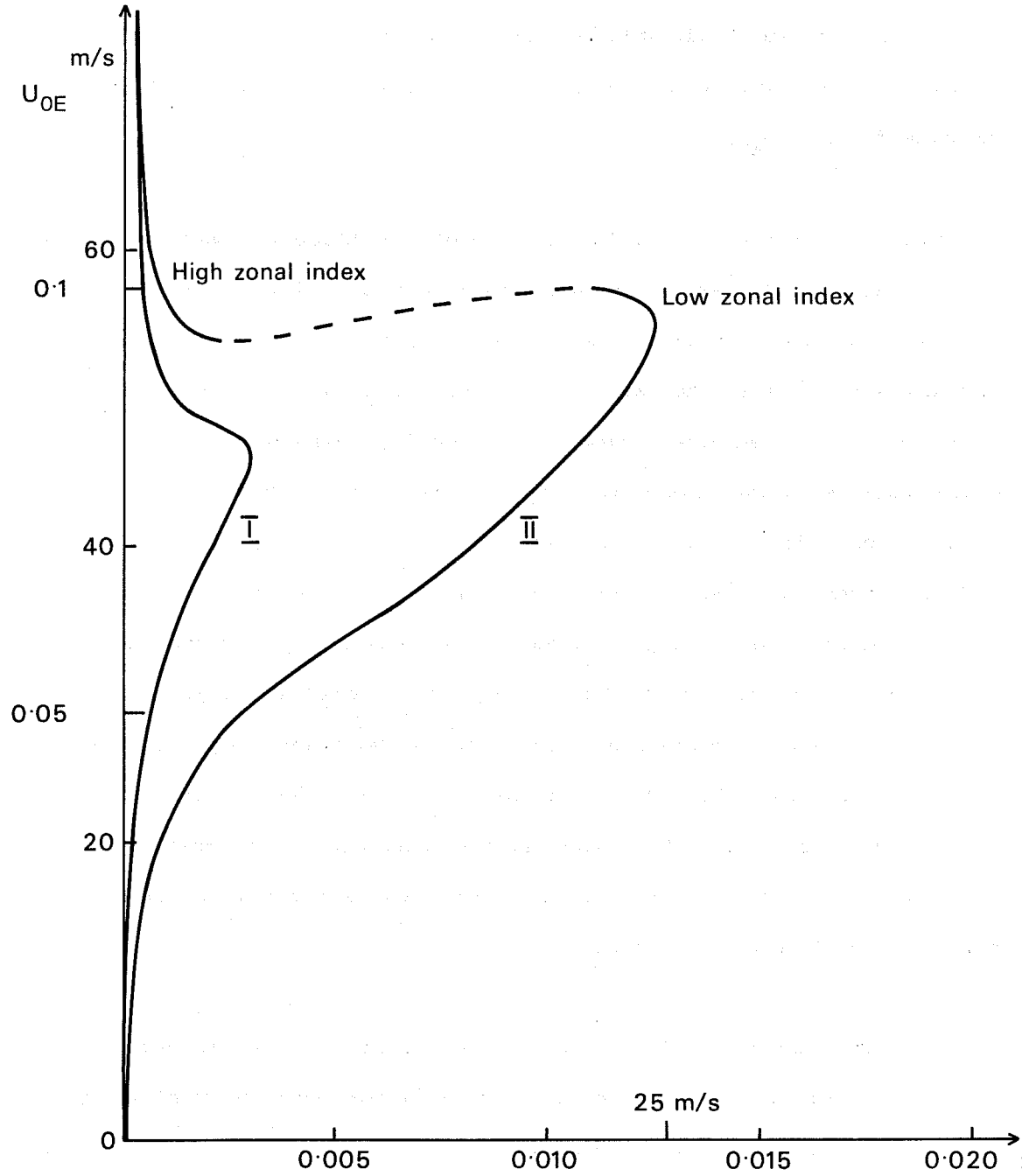

Fig. 2 Steady-state curves for the low order model of section 3. The abscissa gives the response in terms of the amplitude of one of the zonal components (z), the ordinate gives the strength of the zonal forcing (u_{oE}). Both axes are given in dimensional and non-dimensional units, the dimensional units being taken as the zonal average at 45° latitude. The height of the orography, h_1 = 0.05 and the dissipation rate, ε = 0.06. For curve I there is no wave vorticity forcing while for curve II there is a wave vorticity forcing in the same component as the orography (ℓ=3, n_1=4). The amplitude of the wave forcing of curve II is x_{1E}= 0., y_{1E}=-0.015 which corresponds to 20 m/s in terms of a zonally averaged absolute value of the meridional wind at 45° latitude and a phase angle of -90°. Stability properties as indicated by dashed (unstable) and full (stable) lines.

leeward side of the highs in the orography. In Källén 1981 it was shown that this phase angle is the most favourable one for bifurcations to occur. The characteristics of the steady-states within the region of multiple equilibria can be found in the example displayed in Fig. 3. The steady-states on the left hand, upper branch of curve II in Fig. 2 have a marked zonal flow and a rather weak wave component as the top flow of Fig. 3. The steady-states on the right-hand branch, on the other hand, have a much stronger wave component and a weaker zonal flow as the bottom flow of Fig. 3. These latter steady-states can be associated with low index atmospheric circulations, i.e. blocking periods, while the steady-states on the left hand branch have the characteristics of a high index, zonal type of circulation. Examining the energetics of these two solution types it was found in Källén (1981) that in the zonal steady-state the orographic influence on the flow was much weaker than in the blocked state. In the blocked state the orography acted to transform zonal kinetic energy into wave kinetic energy in a much more intense way than in the zonal state. Furthermore, the efficiency of the flow in picking up energy from the wave vorticity forcing was markedly different. In the blocked flow the phase difference between the forced wave and the wave forcing is very small, thus giving a high amplitude response. In the zonal steady state the trough on the leeward side of the orography is further downstream from the orographic high than in the blocked case, and the response amplitude is thus lower. The unstable steady-states on the dashed part of curve II have properties somewhere intermediate between the two stable branch steady-states. The unstable steady-states are, of course, not very interesting. Because of their instability the flow will never settle into them.

It has thus been demonstrated that a combination of orographic and wave vorticity forcing can give rise to multiple equilibrium states, even when the separate effects of the two types of forcing do not show this type of

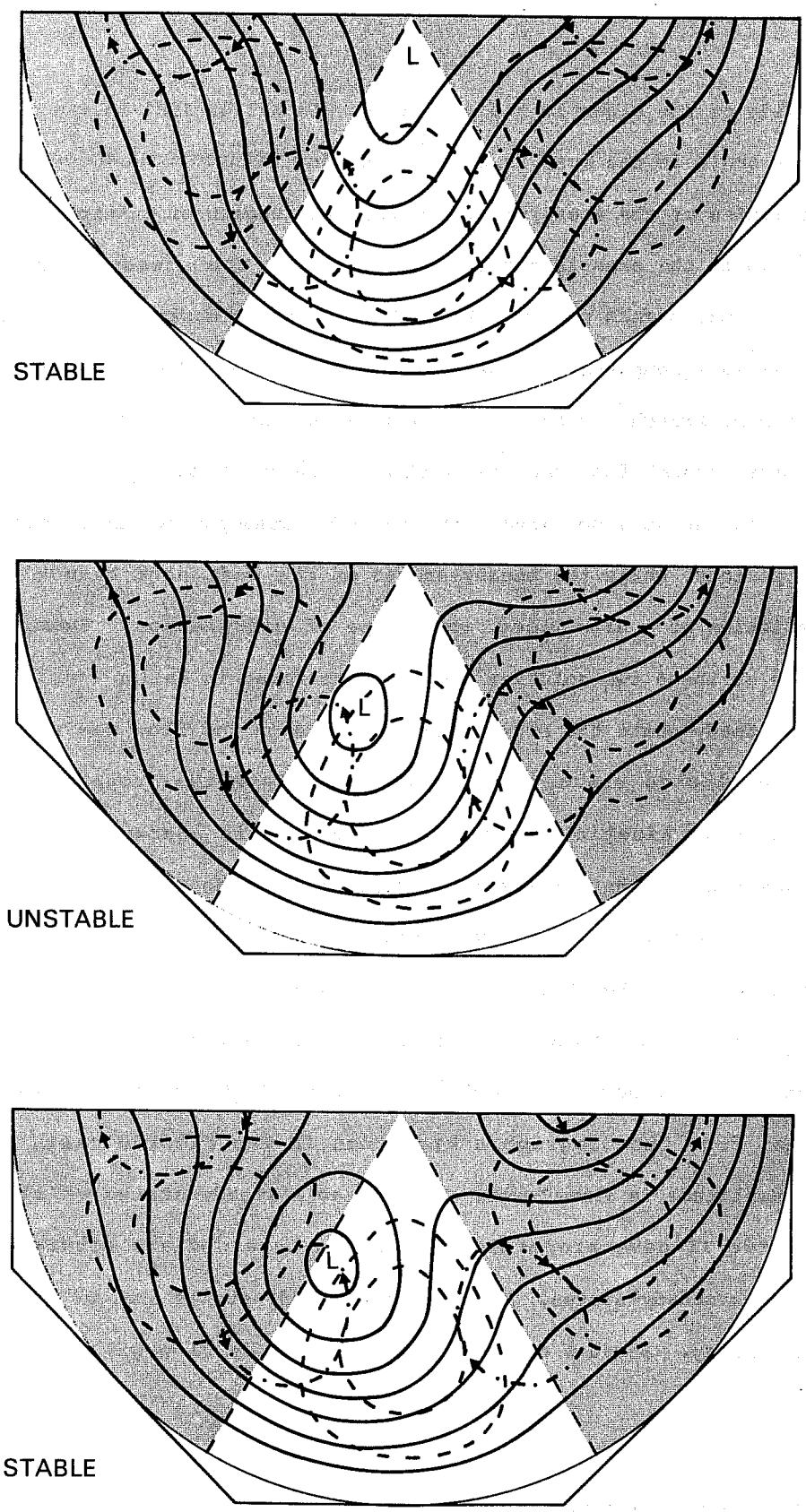

Fig. 3 Examples of stream function fields for three steady-states within the region of possible multiple equilibria of Fig. 2 (curve II). Full lines are isolines of the streamfunction while the dashed lines are isolines for the orography. Over the hatched area the orography is above its mean value ("land areas") while otherwise it is below its mean value ("ocean area"). Dash-dotted curves with arrows showing direction of circulation indicate regions with maximum cyclonic and anti-cyclonic wave vorticity forcing.

behaviour. Only a wave vorticity forcing in this model does not give rise to more than one equilibrium state. The orography can be seen to act as a triggering mechanism, directing the basically vorticity forced flow into one or the other of the stable equilibria.

4. HIGH RESOLUTION EXPERIMENTS

A serious shortcoming of a severely truncated low order system is of course the lack of interaction between waves of all scales. Only a few scales of motion are taken into account and the interactions with other scales are either neglected completely or included via a bulk momentum forcing. To investigate whether the bifurcation mechanism found in a low order model is sensitive to the number of waves present in the model, the results should in some way be verified with a high resolution model. CdV showed that the multiple equilibria in their β-plane channel model could also be found in a model with an increased resolution, while (Davey 1981) pointed out that it is possible to find the multiple equilibria in a high resolution model but they do not obtain as easily as in a low order model.

To verify the results of Källén (1981) for a spherical geometry, experiments have been performed with a high resolution, quasi-geostrophic, spectral, barotropic model. These experiments will be described here following Källén (1982).

The high resolution model was originally developed at the University of Reading, UK and it is a barotropic and quasi-geostrophically balanced version of the model described in Hoskins and Simmons (1975). The governing equation of the model is the same as in Section 2, i.e. Eq.(1). Forcing is introduced in exactly the same components as in the low-order model of Section 3 and the model is integrated in time to find the steady-state(s). For reasons of economy, most of the experiments were done with a T21 truncation ($k \leqslant 21$ and $n \leqslant 21$ in the Legendre ($P_n^k(\mu)$) representation).

However, some integrations done with a T42 truncation showed no significant differences to the T21 experiments.

To find multiple stable steady-states the time integrations are set up in the following manner. Initially the forcing is held constant for a time period of twenty days. The model, starting from a state of rest, is allowed this time to find a steady-state. After the model has settled into a steady-state the zonal momentum forcing is slowly increased or decreased in time. The time scale of this slow increase or decrease is chosen to be significantly slower than the dissipation time scale of the model (the forcing is doubled or halved in 100 days while the dissipation time scale is around 2.5 days). In this way it is hoped that the model stays reasonably close to a stable steady-state all of the time. If, however, a bifurcation of the type pictured in Fig. 2 occurs, the model has to make a sudden jump from one stable branch of the steady-state curve to the other when a critical value in the zonal forcing is passed. In a time plot of some of the spectral coefficients this will show up as a sudden change of the amplitude and perhaps some damped oscillations when the model settles into a steady-state on the other branch.

Results of experiments of this type are displayed in Fig. 4. The forcing parameters have values which are close to the ones used in the low order example of Fig. 2. The phase difference between the wave vorticity forcing and the orography is exactly the same, -90°. It was, however, found that in order to obtain multiple equilibrium states with a high resolution model the vorticity forcing has to be higher. This is presumably due to the fact that the existence of more components forces the energy introduced at certain wave components to spread out to all parts of the spectrum. The long waves, therefore need more energy input to reach the critical amplitudes necessary for bifurcations to occur. The orography, on the other hand, had to be

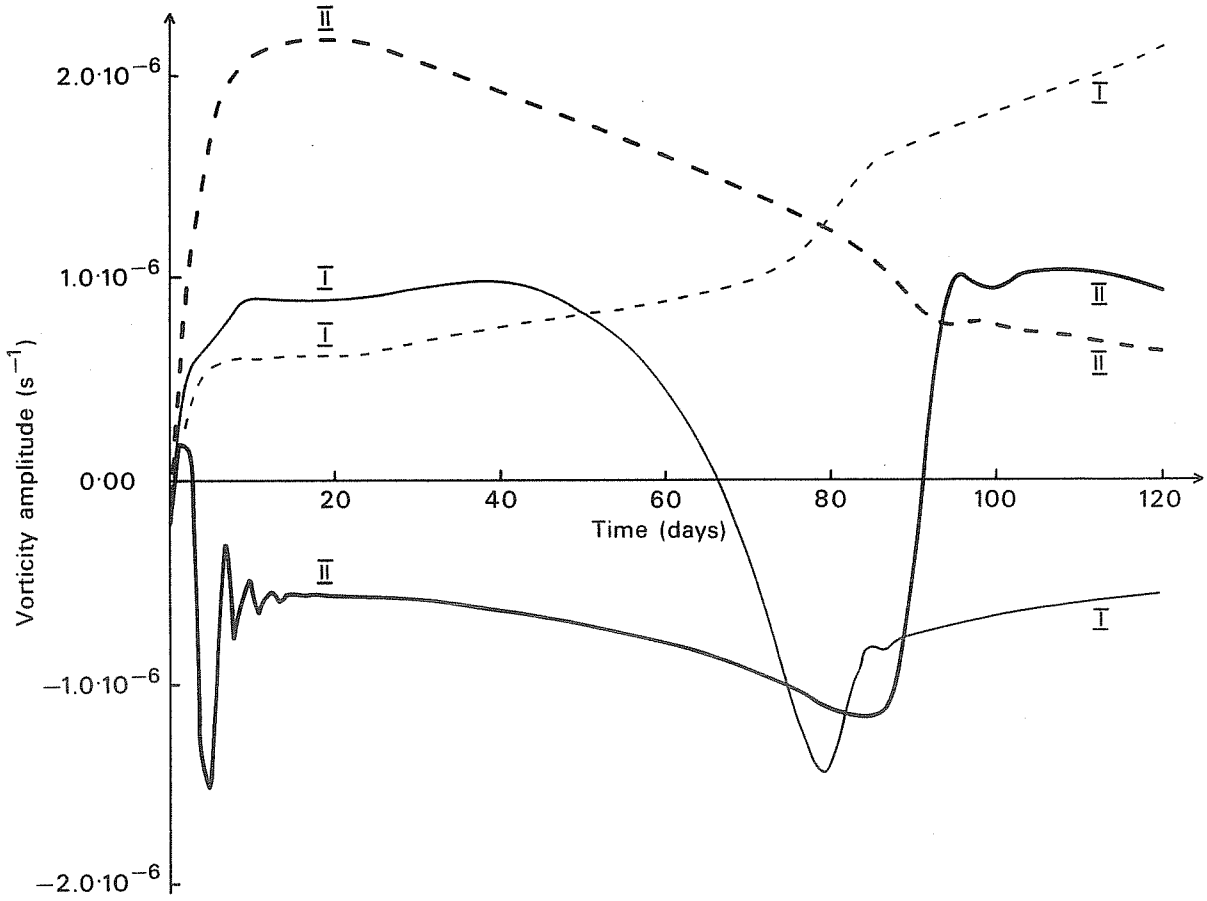

Fig. 4 Vorticity amplitudes of one wave component (k=3, n=4; solid curves) and one zonal component (k=0, n=1; dashed curves) as a function of time in the high resolution model. Curves marked I refer to the experiment with increasing zonal forcing, the ones marked II to a decreasing zonal forcing.
(ε = 0.06, h = 0.025, x_{1E} = 0., y_{1E} = -0.02,

u_{0E} = $\begin{matrix} 0.05 + \\ 0.15 - \end{matrix}$ (time-20)*0.001, time in days).

lowered to avoid the formation of multiple equilibria when only zonal momentum forcing is present. The high resolution model thus appears to be more sensitive to the height of the orography than the low order model.

In Fig. 4 the amplitudes of the forced zonal and wave components are shown as functions of time for two different experiments. In one experiment (curves marked I) the zonal forcing starts at a fairly low value, well below the bifurcation "knee" of the curve in Fig.2. After day 20 the zonal forcing is increased slowly and from the amplitudes of the forced zonal component and the forced wave component it can be seen that a sudden jump occurs around day 80. The curves marked II show a similar experiment, but this time the zonal forcing is decreasing as a function of time. In these curves the jump occurs around day 90 and it should be noted that the jump does not occur at the same value of the zonal forcing as for the jump with an increasing zonal forcing. This strongly suggests that there is a certain interval in the values of the zonal forcing where multiple stable steady-states are possible. To find these steady-states the same type of integrations have been performed, but instead of increasing/decreasing the zonal forcing until the end of the integration the zonal forcing was held constant at a certain level after an increase/decrease from an initially low/high value. The final level of the forcing was chosen to be in the range of possible multiple equilibria. In Fig. 5 the resulting streamfunctions from such an experiment are displayed. The top figure is the steady-state which is reached from an initially high value of the zonal forcing, the lower part is the steady-state reached from an initially low value of the zonal forcing. Comparing these figures with the low order results of Fig. 3 it may be concluded that the streampatterns are qualitatively similar. One has a pronounced wave component and can be interpreted as a blocked steady-state. The other has a much more marked zonal flow and a weaker wave component. The feature displayed in Fig. 2 and shown in Källén (1981) that when orography alone is not sufficient to produce a forcing regime with multiple equilibria, a combination of orographic and

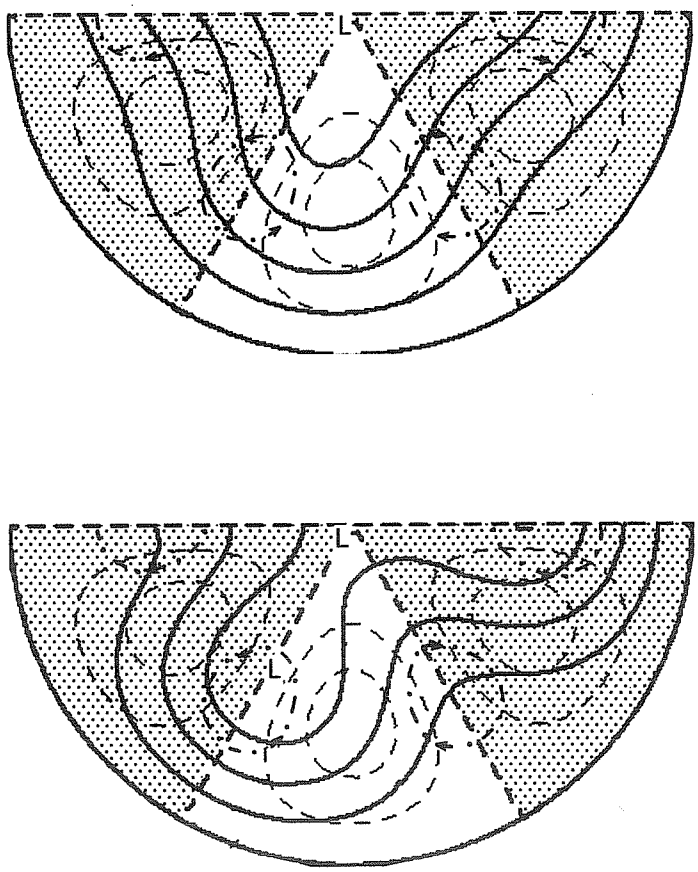

Fig. 5 Two stable streamfunction patterns having the same values of all the forcing parameters ($\varepsilon = 0.06$, $h = 0.025$, $x_{1E} = 0.0$, $y_{1E} = -0.02$, $u_{0E} = 0.095$). Full lines are isolines for the streamfunction with the same isoline interval in the two plots. Dashed lines are isolines for the orography, areas with the orography above its mean value (land areas) are hatched. The dashed-dotted curves indicate the positions and directions of maximum and minimum wave vorticity forcing.

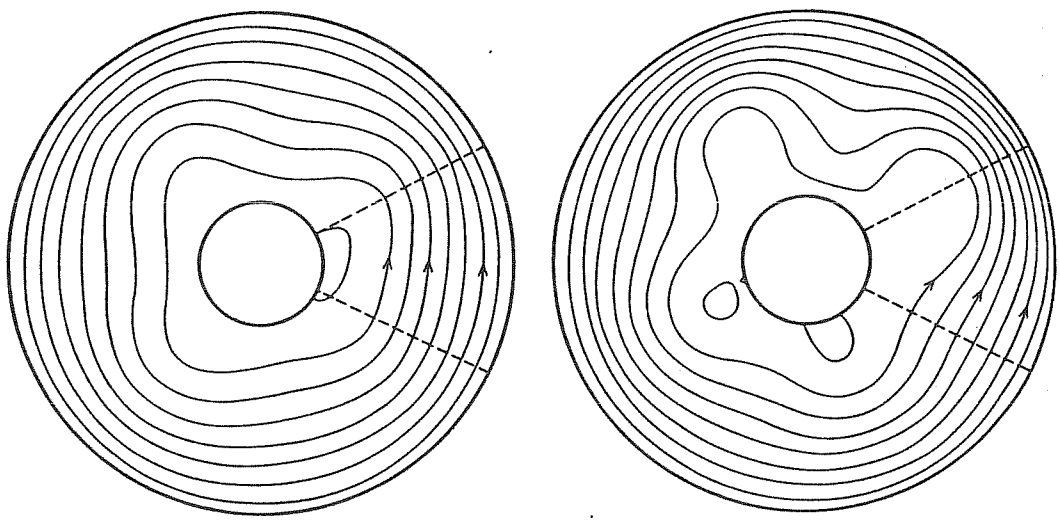

Fig. 6 Alternative stable states in an annular model with an isolated orographic ridge, taken from Davey (1981). Orographic ridge in the right hand sector between the two dashed lines. Full lines are isolines of the streamfunction.

wave vorticity forcing does give this possibility, is reproduced by the high resolution model. The addition of wave vorticity forcing is thus not just a linear addition of wave energy to the flow, instead it actively takes part in the nonlinear formation of multiple equilibria.

The numerical experiments with the high resolution spectral model thus strongly support the results derived from the low order model of Källén (1981). There are, however some aspects of the low order model behaviour which are not verified by the high resolution experiments. One such behaviour is the bifurcation obtained in a low order model in the absence of orography. With a low order model it is possible to find multiple equilibria with only vorticity forcing (Wiin-Nielsen, 1979) on the longer waves. Experiments with the high resolution model have not shown this feature, even for very large values of the forcing parameters. The model behaves perfectly linear when only momentum forcing is applied, the response to the forcing being purely in the forced components. For shorter waves this is no longer true. Hoskins (1973) has demonstrated that for zonal wavenumbers larger than five a nonlinear instability develops which is mainly due to wave-wave interactions. For the longer waves the Coriolis effect acts as a stabilizing factor which prevents this type of nonlinear instability. With orography present it thus seems that a new type of instability develops as first pointed out by CdV. An intuitive reasoning which points to a possible reason for this property of the orography can be given as follows. The governing equation of the model at a steady-state may be written

$$J(\zeta,\psi) + J(h,\psi) - 2\frac{\partial\psi}{\partial\lambda} + \varepsilon(\zeta_E - \zeta) = 0 \qquad (8)$$

If h=0 (no orographic forcing) and $\zeta_E \neq 0$ it is possible to have a steady-state where the response is in the same component as the forcing and the nonlinear term $J(\zeta,\psi)$ is zero. As mentioned above, numerical experiments with

reasonable values of the vorticity forcing on the longer waves have shown that such a steady-state is stable. Equation (8) is in this case linear. This also holds if the wave vorticity forcing is applied at several low wave numbers simultaneously. If an orographic forcing is introduced ($h \neq 0$) the term $J(h,\psi)$ forces energy introduced via the vorticity forcing ζ_E at a certain wavenumber to spread over the whole spectrum. It is this energy spread combined with a suitable vorticity forcing that appears to give rise to a nonlinear instability and the bifurcation leading to multiple steady-states. The experiments with the high resolution model have also confirmed that a suitably positioned vorticity forcing in a wave component enhances this bifurcation mechanism.

Another aspect of using one Fourier component to represent the orography which can be tested with a high resolution model, is to see whether multiple equilibria can be obtained with an isolated orographic ridge. Davey (1981) did an experiment of this type with an annular geometry and within a certain, rather narrow, range of the forcing parameter space, he obtained multiple steady-states. An example of two stable states can be found in Fig. 6. These states have the same characteristics as the blocked and zonal states described previously. It can also be seen from Fig. 6 that in the high amplitude wave state the waves generated on the leeward side of the orographic ridge are almost totally dissipated when the flow reaches the upwind side of the orographic ridge. The high amplitude wave state is thus not associated with a global resonance, the phenomenon is rather local in character. The resonance occurring is instead of the type where the Rossby wave generated by the orography has a phase speed which is such that it is stationary in the zonal flow which results.

5. OBSERVATIONAL STUDIES SUPPORTING A BIFURCATION MECHANISM FOR BLOCKING

The main conclusion that can be drawn from the bifurcation mechanism found in barotropic models is that the orography is necessary as a triggering mechanism in establishing the multiple steady-states. The implied application of the theory to atmospheric blocking can thus be tested by studying the effect of the orography on the atmospheric flow in connection with blocked flow situations. One parameter which reflects the influence of the orography on the barotropic component of atmospheric flow is the mountain torque. To furthermore couple observational evidence with the combination of orographic and wave vorticity forcing, an evaluation of the long wave forcing is needed. This forcing should be seen as the cumulative effect of the transient eddies on the mean flow rather than a direct thermal forcing.

To study the orographic factors influencing blocking action in the Atlantic and Pacific regions separately it is necessary to separate the torque contributions from the American and the Eur-Asian continents. It is primarily downstream from a mountain range that the orography may influence the flow pattern. The mountain torque parameter essentially reflects the surface pressure distribution around a mountain range and therefore it would be possible to separate the contributions from each continent by computing the torque for the eastern and western parts of the Northern Hemisphere separately. The separation line between eastern and western parts would then have to lie entirely within the oceanic regions. Computations of the mountain torque around complete latitute circles has previously been done by Oort and Bowman (1974). They presented monthly averaged results for a five year period including the anomalous winter of 1963. In January 1963 there was a well developed blocking ridge over the Atlantic region (see O'Connor, 1963) and for this month there was an exceptionally high mountain drag in midlatitudes. Recent calculations by Metz (private communication) have also shown a correlation between high values of the mountain drag (again around complete latitude circles) and high amplitudes of the geopotential over the

eastern Atlantic area.

Separating the torque contributions from the North American and the Eur-Asian continents, Källén (1982) has shown that during one winter period (January-March, 1979) there is a correspondence between a mountain drag and the occurrence of a blocking ridge downstream of the mountain barrier.

The mountain drag, T_M, is defined as

$$T_M = - \int_A P_s \frac{\partial h}{\partial \lambda} a \cos\phi \, dS \qquad (9)$$

where p_s is the surface pressure, h the surface elevation above sea level, a the radius of the earth and ϕ, λ the latitudinal and longitudinal coordinates, respectively. The integration is carried out over two areas, one containing the North American continent and another containing the Eur-Asian continent. Both areas extend from the North Pole down to 30°N. The separation lines between the two areas lie entirely within oceanic regions and the torque contributions from both continents can thus be evaluated separately (Fig. 7). A time plot of the torque for the two areas is shown in Fig. 8. The time evolution of the mountain torque has been smoothed with a five day running time mean to remove the influence of short lived, travelling baroclinic eddies. These tend to give large variations in the torque on a time scale of one day.

The most prominent feature of the curves in Fig. 8 is the large variation of the torque on a time scale of about two weeks. Both curves tend to show sudden jumps between what appears to be fairly constant values, the jumps appearing over a time interval which is shorter than the time scale over which the torque is approximately constant. To investigate whether there is

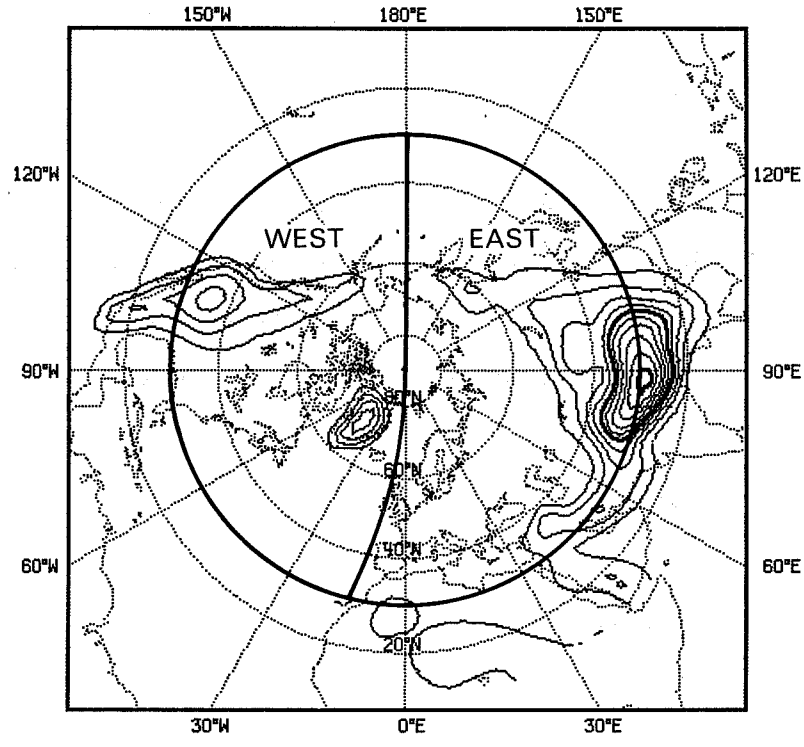

Fig. 7 Geographical map of the orographic field used to calculate the mountain torque. Contours are drawn with a 500 m interval. Thick lines indicate the boundaries of the western and eastern regions used for the calculation of the separate contributions to the mountain torque.

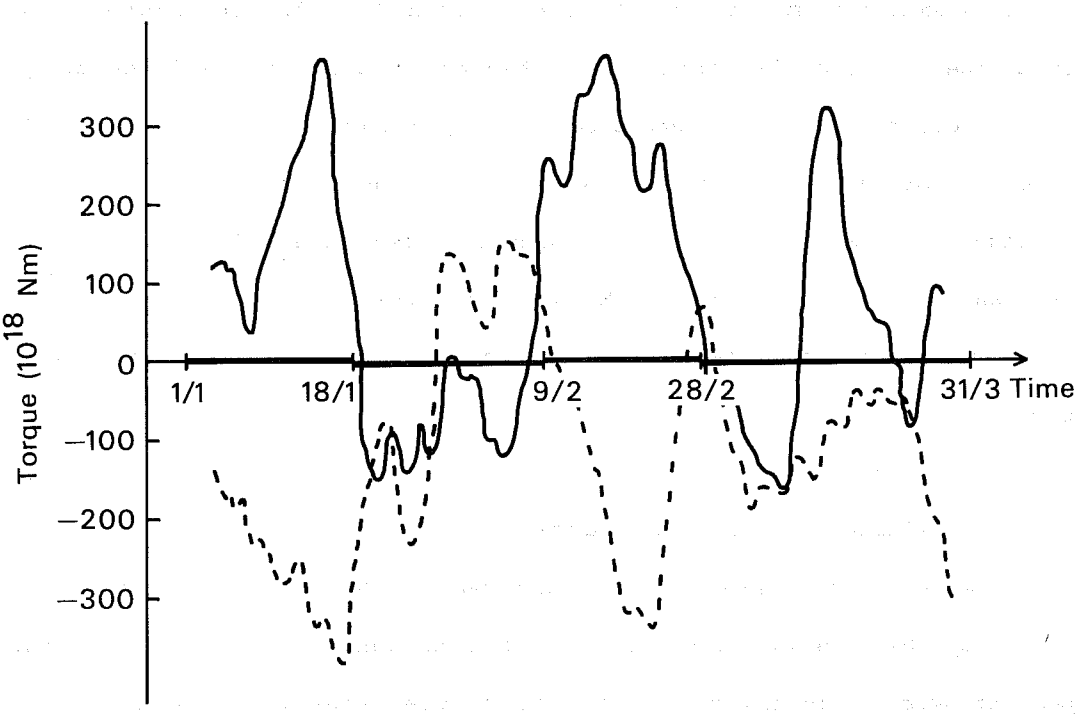

Fig. 8 Mountain torque for western (full line) and eastern (dashed line) parts of Northern Hemisphere (30°N-90°N) during January-March, 1979. The curves are calculated from 12 hourly FGGE data and a running 5-day mean time filter has been applied to smooth the curves. The time periods which are used as averaging periods for Fig. 9 are indicated on the horizontal time axis.

any relation between the periods of low values of the torque (negative values of the torque imply a mountain drag) and the blocking events during January-March 1979, time mean maps of the 500 mb flow have been prepared for the time periods indicated in Fig. 8. The time periods are chosen to coincide with the periods between the jumps in Fig. 9. Also shown in Fig. 9 are areas with a high value of the time variability of the 500 mb surface height. The variability is calculated as the standard deviation of the 12-hourly values from the period average. A high variability indicates an intense eddy activity which can be coupled to strong baroclinic developments at mid-latitudes. A time plot of the variability averaged over regions upstream of the characteristic blocking regions is shown in Fig. 10. The variability in this figure is calculated as the standard deviation from a running seven day average of the 500 mb surface height. A high value of this quantity may thus be interpreted as an intense activity of eddies with a characteristic life time which is between 12 hours and seven days.

The time series has been divided into the following four periods.

I. 1 Jan 1979 - 18 Jan 1979

II. 18 Jan 1979 - 9 Feb 1979

III. 9 Feb 1979 - 28 Feb 1979

IV. 28 Feb 1979 - 31 Mar 1979

During periods I and III there are well developed ridges over the Pacific Ocean and the ridge in period III has many of the characteristics of a blocked flow. In the Atlantic region there is a well developed block during period II while there is a tendency for some ridging over Europe during period III. During period IV there is a predominantly zonal flow over the Atlantic-European region while over the Pacific there is a strong ridge in the poleward part of the region while the flow is zonal across the central Pacific Ocean. Going back to the plot of the mountain torque (Fig. 8), one may see that the Atlantic block during period II and the Pacific block during

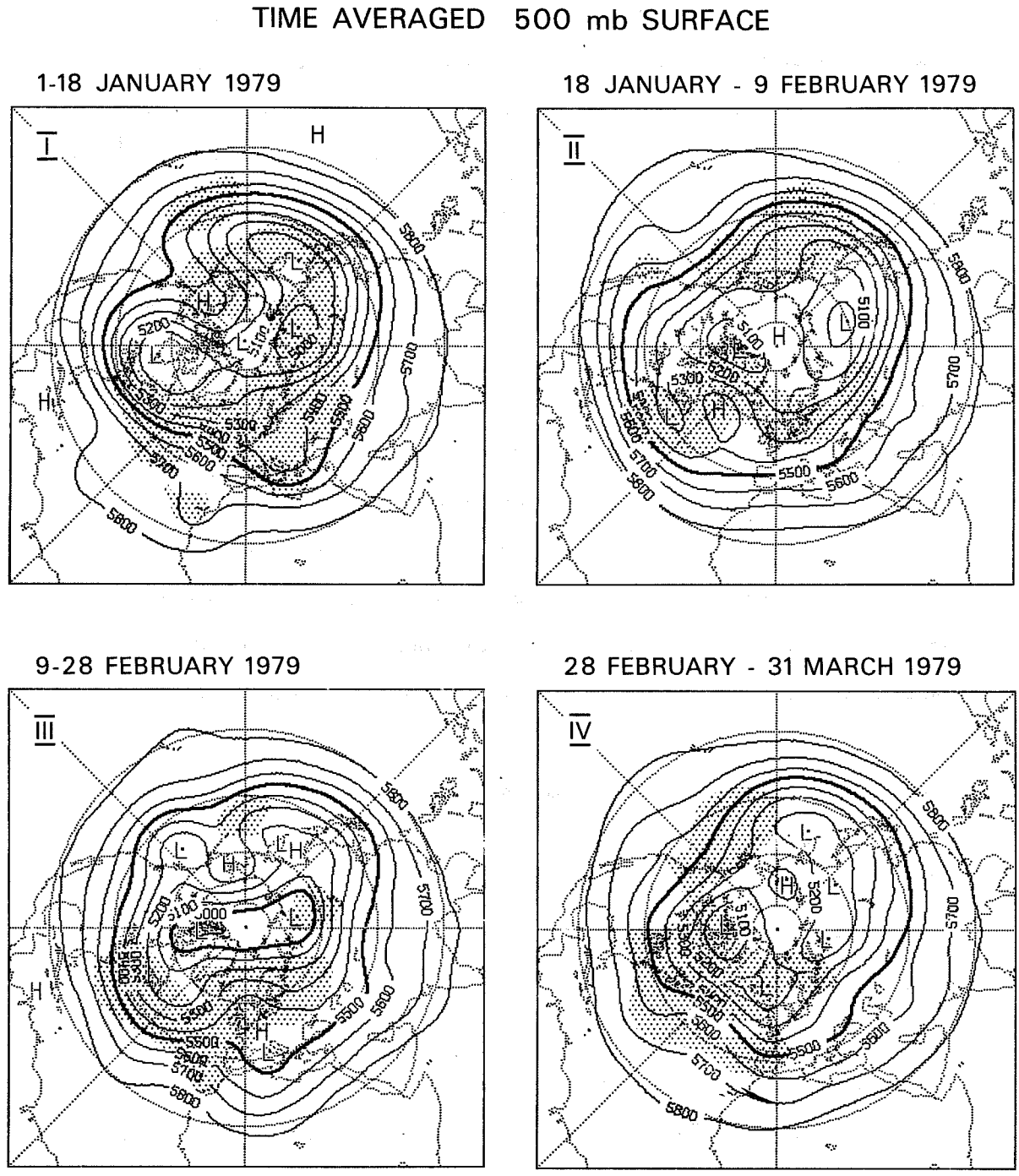

Fig. 9 Time mean maps of the 500 mb surface for the time periods indicated in Fig. 8. Areas where the variance is above 120^2 m^2 are hatched.

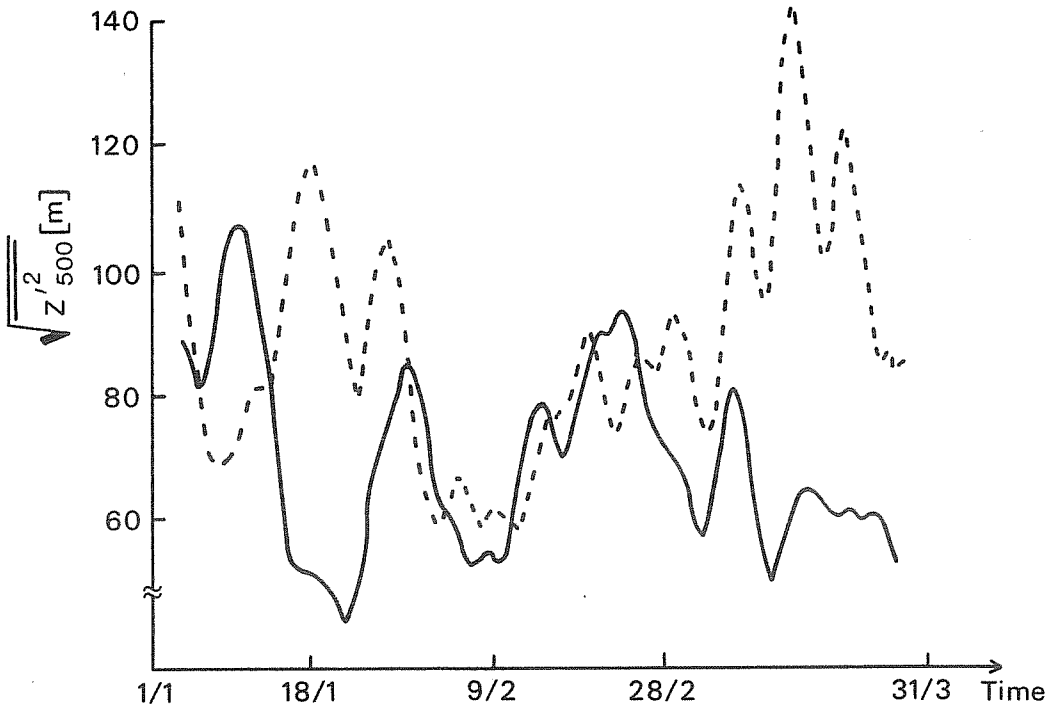

Fig. 10 Time evolution of variances as calculated from deviations of the 500 mb surface from a seven day running mean and spatially averaged over certain regions. All regions extend from 30°N to the North Pole and have the following longitudinal boundaries:

Full line, 135°E - 180°E (Kuroshio region of Pacific Ocean)

Dashed line, 45°W - 90°W (Gulfstream region of Atlantic Ocean).

period III are coupled with low, negative values of the torque, i.e. a mountain drag. The Pacific ridge during period I is also associated with a high mountain drag over the Eur-Asian continent while the zonal flows over the Atlantic region during periods I and III and over the Pacific during period II are coupled with high, positive values of the torque. During the last period (IV) the torque from the North American continent shows considerable fluctuations and the flow over the Atlantic and European regions is predominantly zonal. The torque from the Eur-Asian continent is distinctly negative and there is a ridge extending northwards towards the polar regions over the Pacific Ocean. The occurrence of a high mountain drag thus has some correspondance with the appearance of a blocking high downstream of a continent.

The influence of the transient motion on the time mean flow is the mechanism which in the barotropic model is represented by a direct vorticity forcing. Evaluating this vorticity forcing from atmospheric data is difficult as discussed by Savijärvi (1978). Some attempts have been made at calculating the vorticity forcing for the time periods indicated in Fig. 8, but the results have generally been noisy and it has been difficult to see any clear pattern. Instead, the eddy activity has been evaluated in terms of the standard deviation of the 500 mb surface during the different time periods. From Fig. 9 it may be seen that the eddy activity upstream of a blocking region has some connection with the time periods defined earlier. Through Fig. 10 it may be seen that the Atlantic blocking during period II and to some extent the Pacific blocking during period III are coupled with a strong eddy activity in the beginning of those periods. However, as the blocking period continues there seems to be a decline in the activity of the eddies, especially during period II and in the Atlantic region. The decay of the block may therefore be coupled with the declining eddy activity, when the block has disappeared there is a renewed intensification of the eddy

activity. This reasoning does not hold with the period III block in the Pacific region, there the blocking is preceded by a very low eddy activity. On the geographical maps (Fig. 9) it may however be seen that there is a small region with a fairly high eddy activity just upstream of the block and it may be that the procedure of averaging the variance over a large area smooths this feature out. In any case, the geographical maps clearly show that the upstream flanks of the blocked regions do have intense eddy activity on the average and this is to be expected from the well known fact that in the Gulfstream and Kuroshio regions of the Atlantic and Pacific Oceans respectively, there is normally an intense baroclinic activity.

The ridge over Europe during period III, which on the daily 500 mb maps can be associated with blocking like patterns, is not connected with a high mountain drag over the American continent. This may be explained by the fact that the ridge is too far downstream from the orography to be significantly influenced by it and the blocking ridges may therefore develop due to some other mechanism. From the plot of the variance of the 500 mb surface (Fig. 7) it may however be noted that within the European area there is quite a large variability during this time period. This can be due to blocking like ridges moving across the area and not remaining stationary which also gives a smoothed ridge on a time averaged map. It may thus be a situation in which transient ridges develop, but because of the orientation of the large scale flow and the effect of the orography, the ridges cannot remain stationary to form a persistent block.

6. DISCUSSION

Investigations of the nonlinear properties of simplified atmospheric models have shown that a combination of orographic and vorticity forcing in barotropic, quasi-geostrophic models gives rise to a long wave instability and the development of multiple, stable equilibrium states. One of these stable states can be associated with a large amplitude wave response, while another has a dominating zonal flow and a less pronounced wave component. The large amplitude wave response (or blocked response) is close to a resonant flow configuration, where the wave response is almost in phase with the wave forcing. The zonal steady state is further removed from resonance and the response in the wave component is much weaker. Instead, due to the changed phase relationship between the wave and the orography, the zonal flow is more intense and the mountain drag is lower. These two types of equilibria can exist for the same values of all the forcing parameters, which one the flow choses is crucially dependent on the initial state of the flow in relation to the unstable steady-state.

The forcing parameters required in the barotropic model for the development of multiple equilibria, can be associated with the conditions present in the Northern Hemisphere during wintertime. A strong zonal flow and an intense baroclinic eddy activity off the eastern coasts of the two major continents can thus be linked with two possible types of response of the long waves in the atmosphere. Once the atmosphere has settled into one of these response types it is likely to remain there for an extended period of time due to the stability of the flow configuration. In one of the response types there is a well developed ridge downstream of a continent and this ridge can be associated with a blocked flow. To remain in this near resonant flow configuration it is also necessary that the eddy activity upstream of the blocking ridge is maintained to give an input of kinetic energy on the long waves. From the diagnostic studies of Källén (1982) it appears that this eddy activity steadily decreases during a blocking event and this may be the

cause for the vanishing of the blocking ridge. A decreased eddy activity would, according to the barotropic mechanism put forward in Section 3, imply that the blocked steady-state vanishes (for a constant zonal forcing) and the flow is forced to settle into a zonal flow configuration. In Fig. 2 this may be visualized as the disappearance of curve II when the flow has settled into a state on the high index branch of curve II. At a critical value of the eddy forcing of the long waves the flow would be forced to transfer to a more zonal type of circulation.

Recent investigations by Lau (1981) and Volmer et al (1981) on the behaviour of the GFDL and ECMWF general circulation models in long time integrations have interesting connections with the bifurcation mechanism discussed here. The data from the long integrations were analysed through an expansion into empirical orthogonal functions. Lau (1981) showed that he could find two characteristic types of wintertime circulations in the Northern Hemisphere, one with a predominantly zonal flow and another with a more pronounced meridional flow. Examining the variance during these two characteristic types of months, Lau (1981) was also able to show that the cyclone tracks over the Pacific and North Atlantic Oceans were very different during these months. During the months with a high zonal index the regions with a high variance extended across the oceans, while during the months with a low zonal index the variance was high only over the eastern parts of the oceans. It thus seems that the model has two different modes of circulation during wintertime in the Northern Hemisphere and the characteristic properties of these modes agree quite well with those of the two stable states found in a simple, low order, barotropic model.

References

Charney, J.G. and DeVore, J.G. 1979 Multiple flow equilibria in the atmosphere and blocking. J.Atmos.Sci., 36, 1205-1216.

Davey, M.K. 1980 A quasi-linear theory for rotating flow over topography. Part I: Steady β-plane channel. J.Fluid Mech., 99, 267-292.

Davey, M.K. 1981 A quasi-linear theory for rotating flow over topography. Part II: Beta-plane annulus. J.Fluid Mech., 103, 297-320.

Hoskins, B.J. 1973 Stability of the Rossby-Haurwits wave. Quart.J.R.Met.Soc., 99, 723-745.

Hoskins, B.J. and Simmons, A.J. 1975 A multi-layer spectral model and the semi implicit method. Quart.J.R.Met.Soc., 101, 637-655.

Källén,E. 1981 The nonlinear effects of orographic and momentum forcing in a low-order,barotropic model. J.Atmos.Sci., 39, 2150-2163.

Källén,E. 1982 Bifurcation properties of quasi-geostrophic, barotropic models and the relation to atmospheric blocking. Tellus, in press.

Lau,N.C. 1981 A diagnostic study of recurrent meteorological anomalies appearing in a 15-year simulation with a GFDL general circulation model. Mon. Wea. Rev., 109, 2287-2311

Lorenz, E.N. 1960 Maximum simplification of the dynamic equations. Tellus, 12, 243-254.

Marsden, J.E. and McCracken, M. 1976 The Hopf bifurcation and its applications. Springer Verlag, New York, pp.408.

O'Connor, J.F. 1963 The weather and circulation of January 1963. Mon.Wea.Rev., 91, 209-218.

Oort, A.H. and Bowman, H.D. 1974 A study of the mountain torque and its interannual variations in the Northern Hemisphere. J.Atmos.Sci., 31, 1974-1982.

Saltzmann, B. 1970 Large-scale atmospheric energetics in wave-number domain. Rev. of Geophysics and Space Physics, 8, 289-302.

Savijärvi, H. 1978 The interaction of the monthly mean flow and large scale transient eddies in two different circulation types, Part II. Geophysica, 14, 207-229.

Steinberg, H.L., Wiin-Nielsen, A. and C.-H. Yang 1971 On nonlinear cascades in large-scale atmospheric flow. J.Geophys.Res., 76, 8629-8640.

Trevisan,A. and Buzzi, A. 1980 Stationary response of barotropic weakly nonlinear Rossby waves to quasi-resonant orographic forcing. J.Atmos.Sci., 37, 947-957.

Volmer, J.P., Deque, M. and Jarraud, M. 1981 Large scale fluctuations in a long range integration of the ECMWF spectral model. Manuscript available from ECMWF.

Wiin-Nielsen, A.C. 1979 Steady states and stability properties of a low order barotropic system with forcing and dissipation. Tellus, 31, 375-386.